

# THE RELATIONSHIP BETWEEN PIGMENT PROPERTIES, PAPER STRUCTURE AND THE SHOW-THROUGH OF PRINTED COLOUR

*Dr Anthony Hiorns*

⊕ KAOLIN

⊕ GCC

⊕ PCC

# THE RELATIONSHIP BETWEEN PIGMENT PROPERTIES, PAPER STRUCTURE AND THE SHOW-THROUGH OF PRINTED COLOUR

Anthony Hiorns  
IMERYS Minerals Ltd  
Pigments for Paper  
Par Moor Centre  
Par  
Cornwall  
PL24 2SQ  
UK  
[Tony.Hiorns@imerys.com](mailto:Tony.Hiorns@imerys.com)

## ABSTRACT

The structure of paper is critical in determining many important properties, such as strength, liquid absorption and optics. The particle size and shape of pigments used as either fillers or in coating can have significant effects on the optical performance of paper. Light scattering of a paper sheet can be measured at many different wavelengths quickly and easily using a modern spectrophotometer. Previous work has shown that smaller particles tend to display large differences in the scattering when going from the blue to red end of the visible spectrum. This change in scattering also means that the opacity of the sheet also reduces with longer wavelengths. Therefore, it was expected that the show-through of various printed colours will be different. It is possible to use the light scatter and absorption data calculated using Kubelka-Munk theory to determine CIE  $L^*$ ,  $a^*$ ,  $b^*$  colour values. The CIE colour strength difference can be calculated when the  $L^*$ ,  $a^*$ ,  $b^*$  values of a stack of unprinted sheets are compared to those from a unprinted sheet over a solid coloured print. Examples are given for pigments both in a coating and as a filler. In a coating layer, there is a cross-over in opacity with wavelength, where smaller particles have higher blue light scattering, but lower red light scattering. This results in smaller particles giving a lower CIE colour difference over inks that are red/yellow (longer wavelength) and larger particles giving a lower CIE colour difference over inks that are blue/green (shorter wavelength). Several aragonitic, rhombohedral and scalenohedral PCC's have been used as fillers in a woodfree paper. Each type of PCC filler shows a slightly different response to colour and a  $0.8\mu\text{m}$  rhombohedral PCC is similar in performance to a  $1.6\mu\text{m}$  aragonitic PCC and a  $2.0\mu\text{m}$  scalenohedral PCC. This is due to the size of the primary particles inside the aggregate relative to the aggregate size. This type of information can be invaluable in product development, when the optical performance of pigments can be optimised. It can be used to obtain higher whiteness, controlled tint and better print performance through reduced show-through.

## BACKGROUND

The physical structure of paper will determine many of its properties, including its interaction with light. The size and shape of pigments used both to fill and coat paper can have a significant effect on the structure and hence the optical performance of the paper. Modern spectrophotometers can output reflectance data over the whole visible spectrum, rather than just a few specific wavelengths associated with older standards (e.g.  $\sim 457\text{nm}$  for brightness and  $\sim 550\text{nm}$  for opacity). This means that it is relatively easy to calculate sheet light scattering ( $S$ ) and absorption ( $K$ ) using Kubelka-Munk equations at a range of different wavelengths ( $\lambda$ ). It has been found that there is a relationship between light scattering and the size of the scattering features, both in paper [1,2] and in other cases, such as atmospheric scattering [3]. The negative gradient of a plot of  $\log(S)$  against  $\log(\lambda)$  indicates the scattering size, with a higher value being associated with smaller scatters. This gradient is sometimes referred to as a wavelength exponent. This can be used to evaluate only relative differences in paper structure because it does not always give an accurate size value. The value of the wavelength exponent varies between 4 and 0. For very small particles, typically less than  $1/15$  of the wavelength of the light used, then Rayleigh scattering occurs, where scattering depends on  $\lambda^{-4}$ . At the other extreme, when the particles are quite large, typically at least 20 times the wavelength of light used, then Mie theory indicates that scattering is largely independent of particle size. The knowledge that, for paper,  $S$  tends to decrease at longer wavelengths means that the opacity of the paper also tends to decrease. This means that the ability of "cover up" different printed colours will depend on the  $S$  v  $\lambda$  relationship of the sheet.

## EXPERIMENTAL DETAILS

A DataColor Elrepho 3300 was used to measure the optical characteristics of the papers using D65/10 illumination and a -420nm UV cut-off filter. To calculate S and K data, the reflection spectra of the sheets need to be measured over a black-trap ( $R_o$ ) and over a stack of sheets ( $R_i$ ). The ratio of these values at a given wavelength is a measure of the opacity of the sheet ( $100 \times R_i/R_o$ ). Kubelka-Munk theory was used to calculate the sheet S and K at 400 to 700 nm in 10 nm steps. The wavelength exponent is the negative gradient of a plot of  $\log(S)$  against  $\log(\lambda)$ , with smaller scatters giving higher values. All papers were conditioned at 50% relative humidity and 23°C for 24 hours before testing.

In Example 1, four experimental rhombohedral precipitated calcium carbonates (PCC) were used. They had similar pigment brightness ( $96.2 \pm 0.1$ ) and similar shaped particle size distributions (see Figure 1). They were applied to a  $60 \text{ g/m}^2$  woodfree base using a short dwell head on a laboratory Helicoater at coat weights of 8 to  $16 \text{ g/m}^2$  per side at 800 m/min at the highest runnable coating solids. The formulation consisted of 9 pph of Dow 920 SBR latex, 2 pph Cargill C\*Film 07311 starch, 0.5 pph Kuraray Mowiol 4-98 PVOH and NaOH was used to adjust the pH to ~9. The papers were calendered using an EnfoPlan EP200 laboratory calender for 1 nip at 200 kN/m pressure and 50°C at 40 m/min. The S and K values for each PCC coating system were calculated from the reflection spectra derived by interpolation to a coat weight of  $12 \text{ g/m}^2$ .

In Example 2, ten experimental PCC fillers (5 scalenohedral, 3 aragonite, 2 rhombohedral) were used to make handsheets of  $80 \text{ g/m}^2$  uncoated woodfree paper at three different filler levels (~20, 25, 30%). The PCC pigment properties are shown in Table 1. An 80/20 blend of birch and kraft fibre was used when refined to 25°SR. 0.15% of BIM Kemisize 200 ASA was used for sizing and added to the filler and then 0.02% of Ciba Percol 292 was added as a retention aid. The filled papers were lightly calendered using an EnfoPlan EP200 laboratory calender at 5 kN/m, 30°C, 40 m/min and 1 nip/side. The S and K values for each PCC filler system were calculated from the reflection spectra derived by interpolation at a basis weight of  $80 \text{ g/m}^2$  and a filler level of 25%.

To provide acceptable print colour values, the print density (see Table 2) and reflectance spectra of the solid printed areas (as shown in Figure 2) from a commercially printed double-coated woodfree paper was measured.

Kubelka-Munk theory was then used to calculate the reflectance spectrum of a given coated or filled sheet over each printed colour, using the reflectance of the coloured print as the substrate reflectance and the S, K and basis weight of the sheet at each wavelength. This reflectance spectrum can then be used to calculate the CIE  $L^*$ ,  $a^*$ ,  $b^*$  colour parameters. An estimate of the colour show-through can be obtained by calculating the degree of colour difference between a stack of unprinted sheets and a sheet over a given printed colour using the CIE colour difference equations. This type of approach has been used to calculate print-through of ink on coloured newsprint [4].

CIE colour difference equation:

$$\Delta E = \sqrt{(L_1^* - L_2^*)^2 + (a_1^* - a_2^*)^2 + (b_1^* - b_2^*)^2}$$

CIE-94 colour difference equation:

$$\Delta E_{94} = \sqrt{(L_1^* - L_2^*)^2 + \left( \frac{C_1^* - C_2^*}{1 + 0.045\sqrt{C_1^* C_2^*}} \right)^2 + \left( \frac{H_1^* - H_2^*}{1 + 0.015\sqrt{C_1^* C_2^*}} \right)^2}$$

Where:

$\Delta E$  is the 1976 CIE colour difference

$\Delta E_{94}$  is the CIE-94 colour difference

1,2 denote values for stack of unprinted sheets and a single unprinted sheet over a printed colour

Colour strength  $C^* = \sqrt{a^{*2} + b^{*2}}$

Hue  $H^* = \arctan(b^* / a^*)$

## RESULTS

### Example 1. Four PCC pigments used for coating.

Figure 3 shows the reflection spectra and opacity of the PCC coated sheets with wavelength. It can be seen that lines for the reflection spectra of the single coated sheets over a black trap cross-over at about 525 nm, with the PCC with the smallest particle size (PCC-1) having a higher reflectance at shorter wavelengths, but a lower reflectance at longer wavelengths. The reflectance spectra for a stack of sheets show a pronounced dip at about 590 nm. This corresponds to a peak in the opacity values and is due to a dye in the base paper. Overall, the trend is for opacity to decrease at longer wavelengths.

Figure 4 shows the calculated S and K values with wavelength for the PCC coated sheets. The S values show a similar pattern as that seen in the single sheet reflectance spectra, but with the cross-over point being about 545 nm. The K values show a large peak at about 580 nm which is due to the dye in the base paper. The effect of the dye in the base paper can be estimated by adjusting the K values to remove this peak, as also shown in Figure 4. Figure 5 shows how the adjustment of the K values has affected the reflectance spectra and opacity with wavelength. The dips and bumps present when dye is in the base (Figure 3) have been replaced by much smoother functions (Figure 5).

Figure 6 shows the CIE  $a^*$  and  $b^*$  values plotted for each of the PCC coated papers over the various printed colours. There is a consistent trend of moving to higher  $a^*$  and higher  $b^*$  when moving from a coating PCC with a mean particle size of 0.40  $\mu\text{m}$  to 0.93  $\mu\text{m}$ . The effect of subtracting the dye in the base is to increase the  $b^*$  value, i.e. a move to a more yellow/less blue sheet.

The CIE and CIE-94 colour difference data between a stack of unprinted sheets and a single sheet over solid coloured prints are shown in Tables 3a and 3b. Plots of the CIE-94 colour differences are shown in Figure 7. The two spider plots allow the effect of dye in the base to be visualised. When dye is present, the colour differences are smaller, i.e. the dye increases light absorption and has an overall opacifying effect. The printed colour that shows the greatest variation is yellow. However, when the effect of the dye in the base paper is removed by calculation, the colour differences are larger and there is less variation for each printed colour. Figure 8 is the spider plot that shows the colour differences with the dye removed from the base paper on an expanded scale. It can now be seen that there are different trends with coating PCC with printed colour. Figures 9a and 9b show the trends between CIE and CIE-94 colour difference and mean particle size. The variations in colour difference are relatively small, but the trends appear to be quite good ( $R^2$  fit values typically  $>0.9$ ) and the slope of these trends can be used to see the effect of particle size on colour show-through (Tables 4a and 4b). There are some minor differences in the order of the inks between the CIE and CIE-94 calculated slope values, but a similar trend with colour exists. For inks with a significant degree of reflection of blue wavelengths (cyan, green, blue), a larger particle size (PCC-4) is better at reducing colour show-through. However, for inks with a high reflection of red wavelengths (red, yellow, magenta), a smaller particle size (PCC-1) is better. One possible explanation for this effect comes from the relationship between particle size, light scatter and wavelength. A smaller particle size has higher scatter of blue light and lower scatter of red light. This means that more of the blue light that would be absorbed by a red or yellow ink will be reflected by the coating, thus helping to reduce the colour difference. This is shown schematically in Figures 10a and 10b.

### Example 2. Ten PCC pigments used for filling.

Figure 11 shows SEM images taken of the PCC fillers. The fillers exhibit an aggregated structure, but the rhombohedral PCC's are less aggregated than either the scalenohedral or aragonitic PCC's. The primary particles making up the aggregates are also much smaller for finest scalenohedral PCC (sPCC A) compared to all of the other pigments. Figures 12a, 12b and 12c show the reflection spectra and opacity of the PCC filled sheets with wavelength. There are large differences in the single sheet reflectance measurement due to particle size, but the reflectance measurements of the stack of sheets show a much smaller effect of particle size. The opacity follows a smooth trend with wavelength, decreasing by about 8 units when moving from the blue to the red end of the visible spectrum. Coarser PCC fillers also tend to give lower opacity than the finer ones. Figures 13a, 13b and 13c show the calculated S and K values with wavelength for the PCC filled sheets. There are only very small differences in sheet K for all of the filler PCC products, indicating that the level of impurities in the PCC is similar, irrespective of size or crystal type. Almost all of the optical differences between the PCC fillers are due to S, with the finer products giving higher S values.

Figure 14 shows the CIE  $a^*$  and  $b^*$  values plotted for each of the PCC filled papers over the various printed colours. Increasing the mean particle size of the PCC filler tends to increase the  $b^*$  value and, to a lesser extent, the  $a^*$  value. However, the effects are much larger for the magenta, red and yellow prints, with the cyan print producing only small changes.

The CIE-94 colour differences between a stack of unprinted sheets and a single sheet over solid coloured prints are shown in Figures 15a and 15b. The spider plots in Figure 15a show that particle size has a major effect of colour show-through, with smaller particles giving reduced show-through. All three PCC crystal types are shown on the same spider plot in Figure 14b. From this plot, it can be seen that there is similar colour show-through given by the 0.8  $\mu\text{m}$  rhombic PCC (rPCC A), the 1.6  $\mu\text{m}$  aragonitic PCC (aPCC B) and the 2.0  $\mu\text{m}$  scalenohedral PCC (sPCC B). These differences in the particle size required for similar opacifying effect are due to the size and shape of the primary particles that make up the aggregate and the overall size of the aggregate.

An indication of aggregate structure may be obtained by plotting the wavelength exponent against the mean particle size, as shown in Figure 16. In this case, the particle size was measured by sedimentation and this requires a density value for the particle ( $\sim 2.7 \text{ g/cm}^3$  for PCC). However, if the particles are aggregated then the density of the aggregate is lower than that of a solid particle and the aggregate will settle slower than expected. Therefore, the value calculated for particle size will be lower than expected. The wavelength exponent gives a relative value that depends on the size of the objects scattering the light and is more likely to represent the primary particles making up the aggregate, rather than the overall aggregate size. It can be seen in Figure 16 that most of the scalenohedral and aragonitic PCC fillers lie on a similar trend. There is a single scalenohedral PCC filler that does lie on the trend (sPCC A). This has much smaller primary particles compared to all of the other aggregated fillers, so has a higher wavelength exponent for a given mean particle size. The rhombohedral PCC fillers lie on a separate trend because they are less aggregated than the other PCC fillers.

## CONCLUSIONS

The particle size and shape of pigments used as either fillers or in coating can have significant effects on the optical performance of paper. The work in this paper extends previous work that showed that light scattering could be used to determine the relative size of objects that scatter light in a paper. Smaller particles tend to display large differences in the scattering when going from the blue to red end of the visible spectrum. This change in scattering with wavelength also means that the opacity of the sheet will be reduced with longer wavelengths. Light scatter and absorption data calculated using Kubelka-Munk theory was used to determine CIE  $L^*$ ,  $a^*$ ,  $b^*$  colour values and colour difference of a stack of unprinted sheets are compared to those from an unprinted sheet over a solid coloured print. Two examples have been given for pigments, one in coating and the other in filling. In a coating layer, there was a cross-over in opacity with wavelength, where smaller particles have higher blue light scattering, but lower red light scattering. This results in smaller particles giving a lower colour difference for inks that are red/yellow (longer wavelengths) and larger particles giving a lower colour difference for inks that are blue/green (shorter wavelength). Different crystal types of PCC filler exhibit a slightly different response to colour, where a 0.8  $\mu\text{m}$  rhombohedral PCC had similar performance compared to a 1.6  $\mu\text{m}$  aragonitic PCC and a 2.0  $\mu\text{m}$  scalenohedral PCC. This is through to be due to the size of the primary particles inside the aggregate relative to the aggregate size. This type of information that relates pigment size, shape and aggregation, to optical performance of the paper can be invaluable in product development, when the optical performance of pigments can be optimised. It can be used to obtain higher whiteness, controlled tint and better print performance through reduced show-through.

## REFERENCES

- [1] Kortum, G., "Reflectance spectroscopy", Springer-Verlag Berlin-Heidelberg, (79-86181), 1969.
- [2] Hiorns, A.G., "Investigating paper structure using light scattering", TAPPI Coating and Graphic Arts Conference, Atlanta, 2006.
- [3] Angstrom, A., "Technique of determining the turbidity of the atmosphere", Tellus, Vol.13, 1961.
- [4] Makinen, M, Jääskeläinen, T., Parkkinen, J., "Evaluation of print-through with colour theory", TAPPI Coating and Graphic Arts Conference, Atlanta, 2006.

Table 1. PCC filler pigment properties

	Pigment Label	PSD Mean Size (D <sub>50</sub> , μm)	Surface Area (m <sup>2</sup> /g)	PSD Steepness (100 · D <sub>30</sub> /D <sub>70</sub> )	Powder Brightness (%)
Scalenohedral PCC	sPCC A	1.5	15.6	69	95.1
	sPCC B	2.0	7.0	68	94.0
	sPCC C	2.4	5.7	66	95.9
	sPCC D	2.5	5.2	69	95.5
	sPCC E	2.6	4.4	66	94.3
Rhombic PCC	rPCC A	0.8	6.8	64	96.8
	rPCC B	1.3	4.4	66	96.7
Aragonitic PCC	aPCC A	0.9	10.6	63	95.3
	aPCC B	1.6	7.5	68	94.1
	aPCC C	2.3	6.0	69	94.3

Table 2. Print densities of solid offset printed areas from commercial printing

Print Area	Measured Print Density			
	Black	Cyan	Magenta	Yellow
Black (100% K)	<b>1.80</b>	1.76	1.82	1.87
Cyan (100% C)	0.76	<b>1.38</b>	0.44	0.21
Magenta (100% M)	0.64	0.25	<b>1.31</b>	0.69
Yellow (100% Y)	0.15	0.11	0.18	<b>0.99</b>
Red (100% M + 100% Y)	0.64	0.24	1.27	1.36
Green (100% C + 100% Y)	0.83	1.31	0.52	0.94
Blue (100% M + 100% C)	1.34	1.32	1.19	0.65

Table 3a. CIE and CIE-94 colour differences for ink show through (dye in base)

	CIE				CIE-94			
	PCC-1	PCC-2	PCC-3	PCC-4	PCC-1	PCC-2	PCC-3	PCC-4
Black	4.62	4.68	4.73	4.72	4.63	4.75	4.89	4.92
Cyan	4.83	4.86	4.89	4.86	4.73	4.80	4.86	4.86
Magenta	4.60	4.69	4.77	4.76	4.38	4.43	4.44	4.44
Yellow	3.13	3.33	3.44	3.49	2.89	3.23	3.61	3.75
Red	4.48	4.58	4.65	4.65	4.25	4.32	4.37	4.39
Green	4.30	4.37	4.41	4.40	4.29	4.37	4.45	4.45
Blue	4.69	4.75	4.79	4.77	4.69	4.80	4.95	4.98

Table 3b. CIE and CIE-94 colour differences for ink show through (no dye in base)

	CIE				CIE-94			
	PCC-1	PCC-2	PCC-3	PCC-4	PCC-1	PCC-2	PCC-3	PCC-4
Black	5.81	5.71	5.66	5.62	5.82	5.82	5.84	5.84
Cyan	6.18	6.08	6.03	5.98	5.33	5.25	5.22	5.19
Magenta	5.56	5.50	5.49	5.47	4.84	4.85	4.88	4.89
Yellow	3.16	3.22	3.27	3.31	4.20	4.25	4.29	4.31
Red	5.37	5.31	5.30	5.28	4.89	4.92	4.96	4.98
Green	5.46	5.36	5.31	5.26	5.22	5.15	5.13	5.09
Blue	5.94	5.84	5.80	5.75	5.80	5.80	5.83	5.85

Table 4a. Effect of PCC mean particle size on colour show-through – from plots of CIE colour difference against mean particle size – no dye in base

	Slope	R <sup>2</sup> fit	Comments
Over cyan (100% C)	-0.366	0.924	Larger D <sub>50</sub> better at opacifying
Over green (100% C + 100% Y)	-0.347	0.920	
Over blue (100% M + 100% C)	-0.347	0.917	
Over black (100% K)	-0.342	0.915	
Over red (100% M + 100% Y)	-0.153	0.850	
Over magenta (100% M)	-0.164	0.857	
Over yellow (100% Y)	+0.271	0.969	Smaller D <sub>50</sub> better at opacifying

Table 4b. Effect of PCC mean particle size on colour show-through – from plots of CIE-94 colour difference against mean particle size – no dye in base

	Slope	R <sup>2</sup> fit	Comments
Over cyan (100% C)	-0.248	0.876	Larger D <sub>50</sub> better at opacifying
Over green (100% C + 100% Y)	-0.222	0.915	
Over black (100% K)	+0.050	0.636	
Over magenta (100% M)	+0.095	0.954	
Over blue (100% M + 100% C)	+0.100	0.865	
Over red (100% M + 100% Y)	+0.164	0.975	
Over yellow (100% Y)	+0.210	0.960	Smaller D <sub>50</sub> better at opacifying

Figure 1. Particle size distributions of the four coating PCC pigments

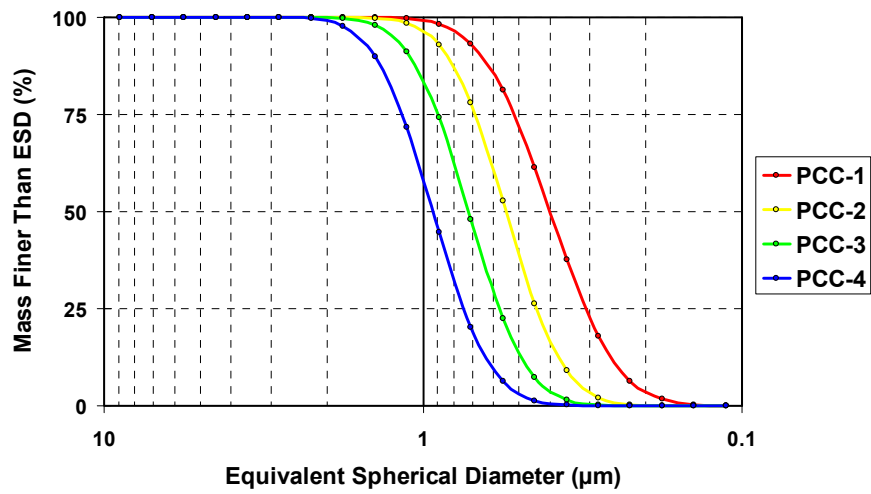


Figure 2. Reflection spectra of solid print areas from commercial printing

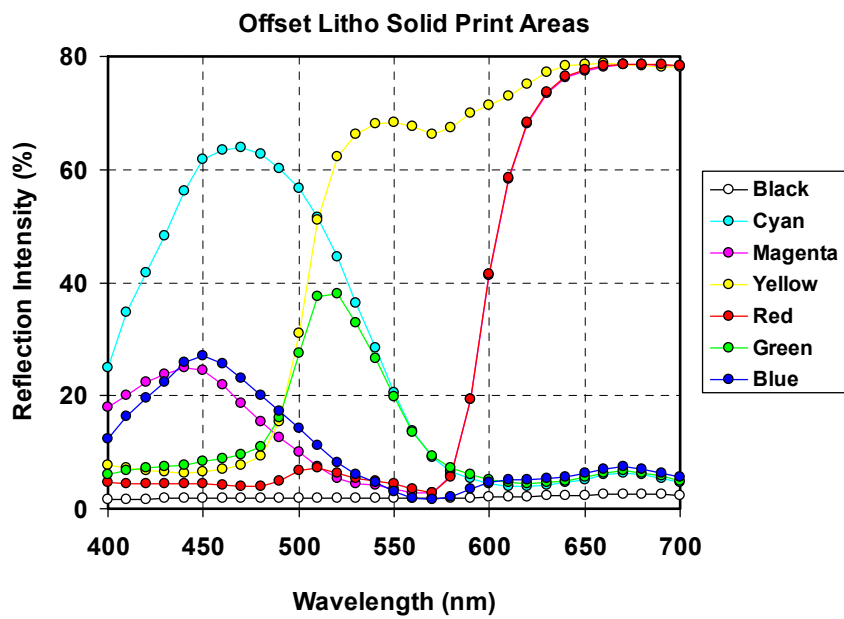


Figure 3. Reflection spectra and opacity of PCC coated sheets

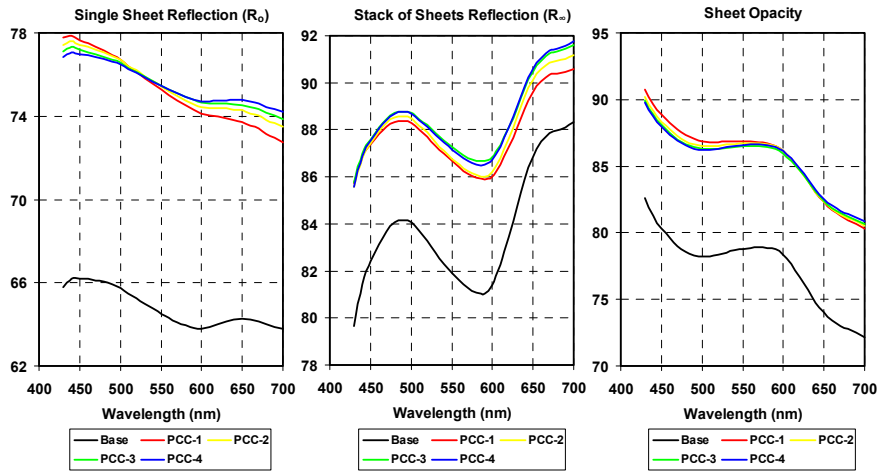


Figure 4. Variation of sheet S and K with wavelength for PCC coated sheets

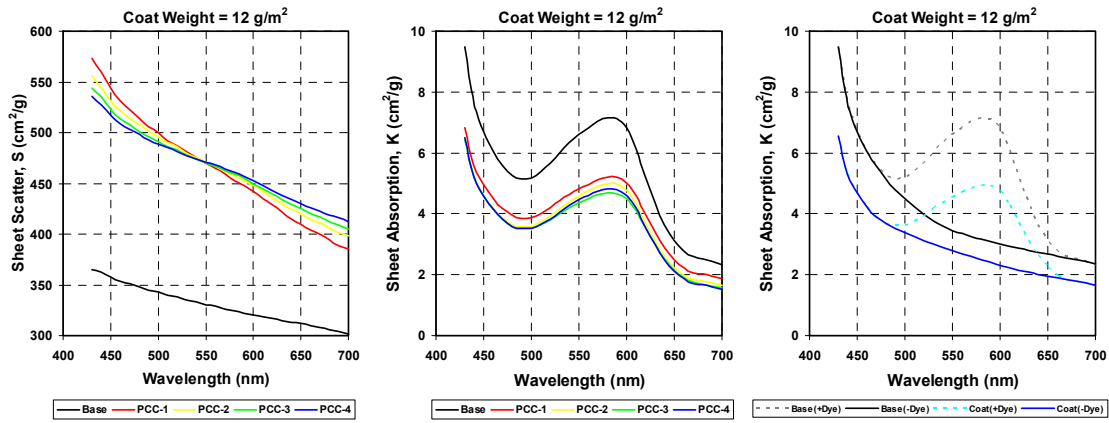


Figure 5. Reflection spectra and opacity of PCC coated sheets with sheet K adjusted to remove effect of dye in the base.

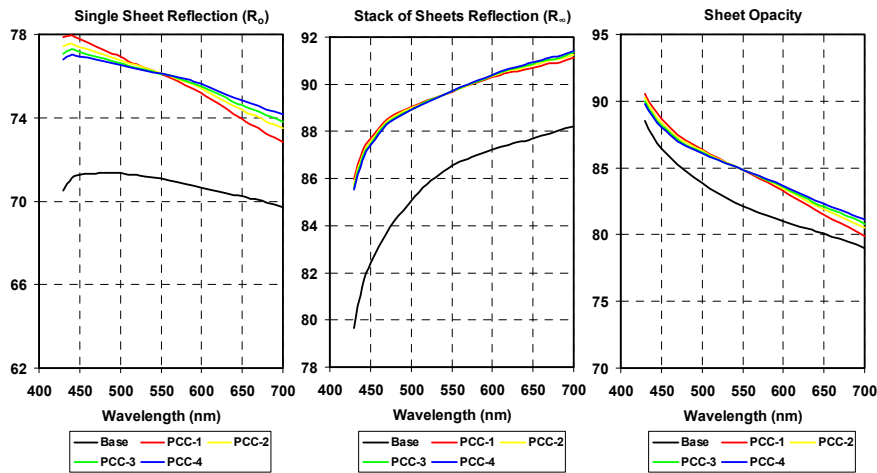


Figure 6. CIE colour parameters for PCC coated paper over solid print areas. The arrows indicate the trends when moving from a coating PCC with a mean particle size of  $0.40\mu\text{m}$  to  $0.93\mu\text{m}$ .

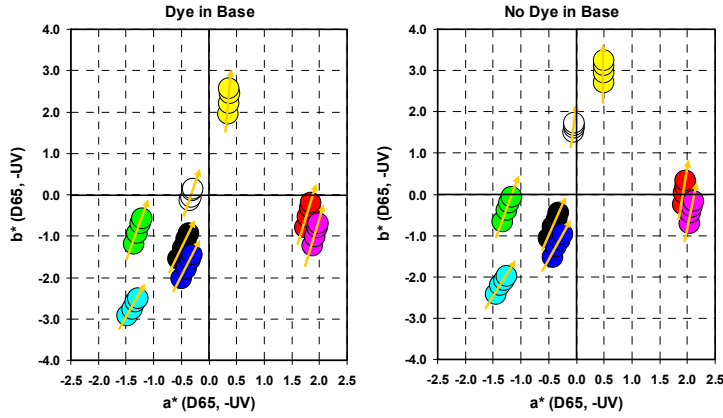


Figure 7 The CIE-94 colour differences of the PCC coated papers over various printed colours with dye present in base paper (left) and dye removed by calculation (right).

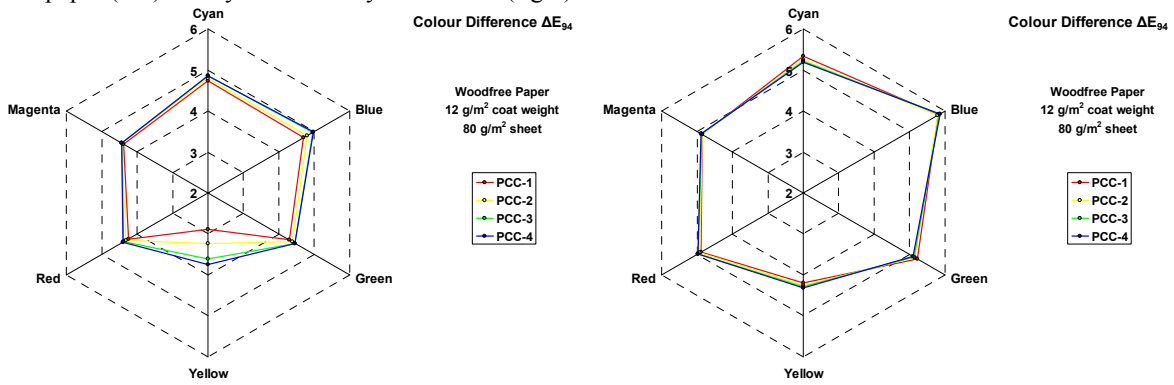


Figure 8. The CIE-94 colour differences of the PCC coated paper over various printed colours with dye removed by calculation (expanded scale).

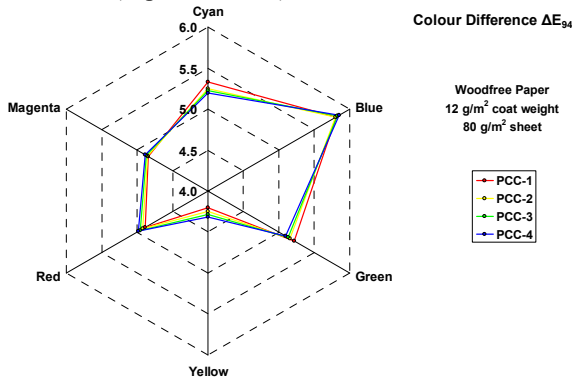


Figure 9a. Relationship between CIE colour difference and PCC coating pigment mean particle size for different printed colours.

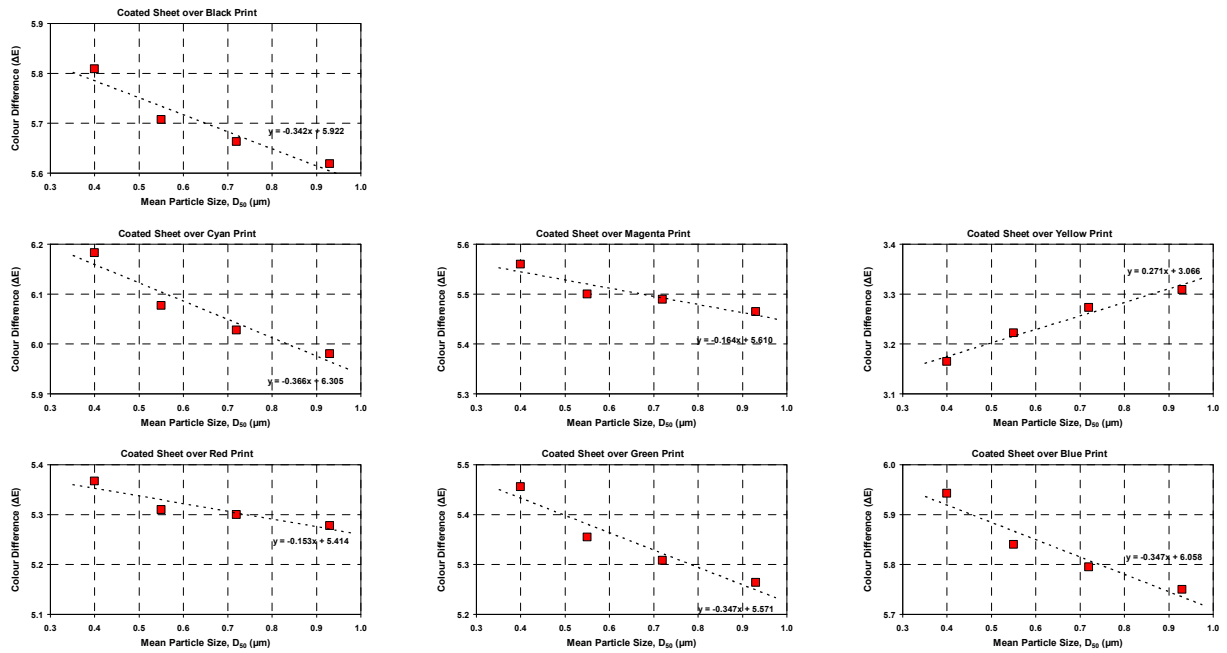


Figure 9b. Relationship between CIE-94 colour difference and PCC coating pigment mean particle size for different printed colours.

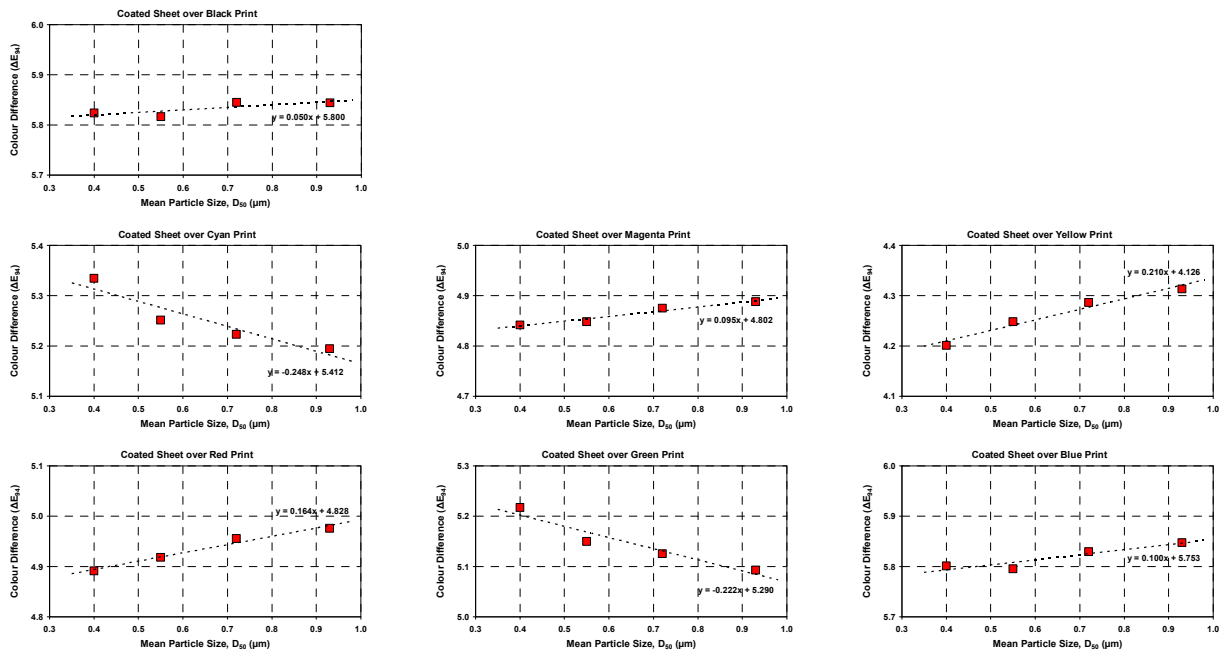


Figure 10a. Schematic diagram of effect of small scatter size in the paper on colour difference

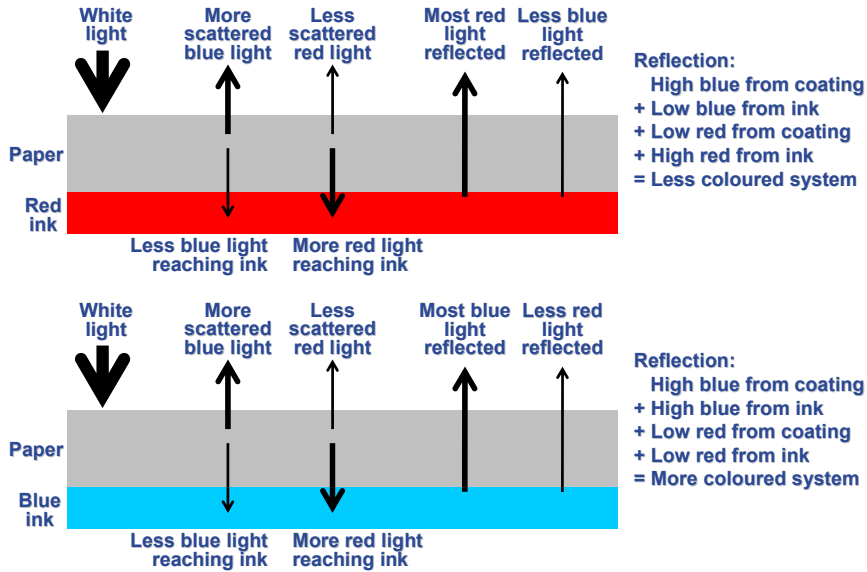


Figure 10b. Schematic diagram of effect of large scatter size in the paper on colour difference

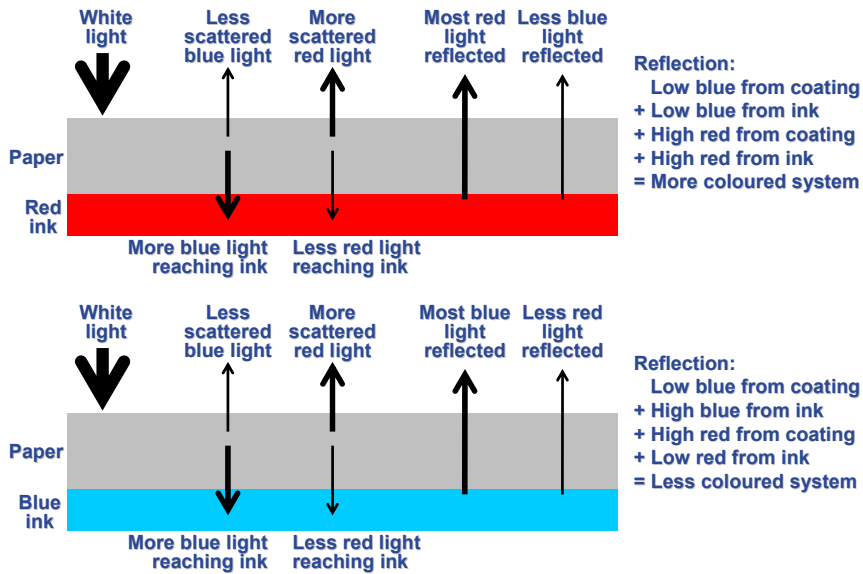
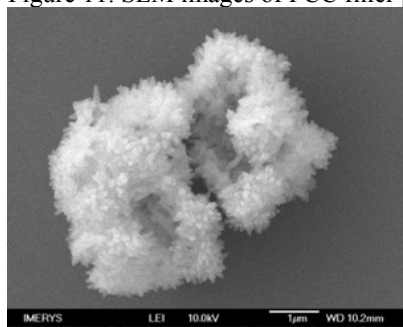
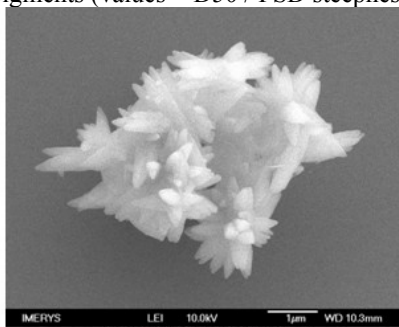


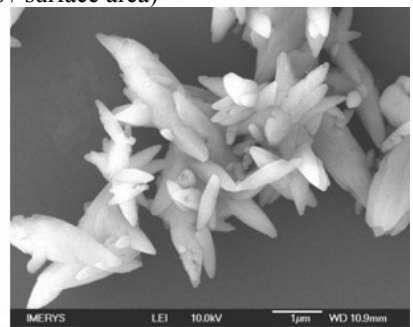
Figure 11. SEM images of PCC filler pigments (values = D50 / PSD steepness / surface area)



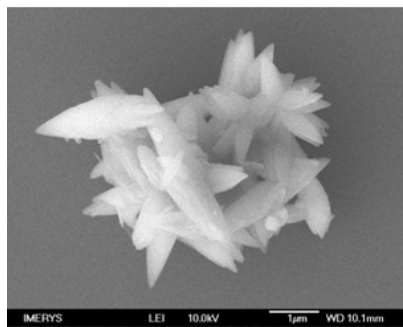
sPCC A (1.5 / 69 / 15.6)



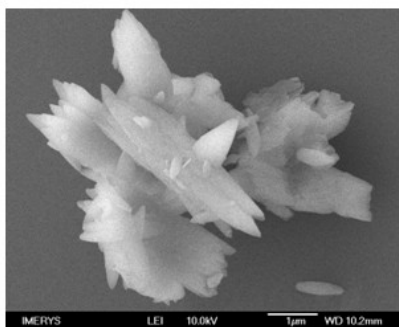
sPCC B (2.0 / 68 / 7.0)



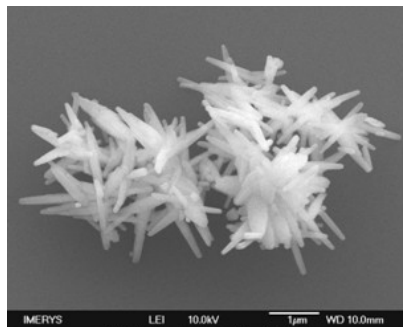
sPCC C (2.4 / 66 / 5.7)



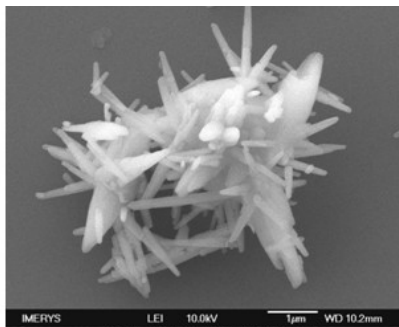
sPCC D (2.5 / 69 / 5.2)



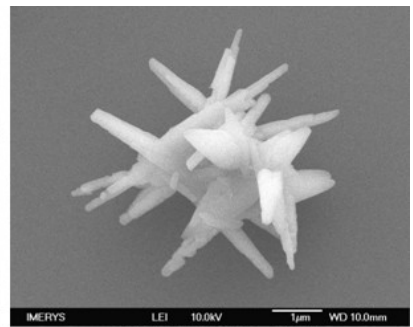
sPCC E (2.6 / 66 / 4.4)



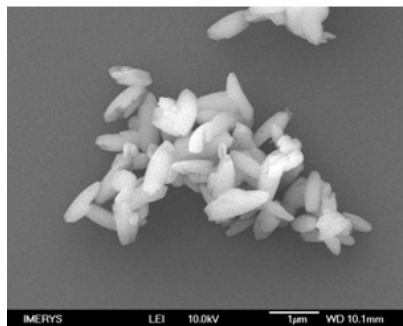
aPCC A (0.9 / 63 / 10.6)



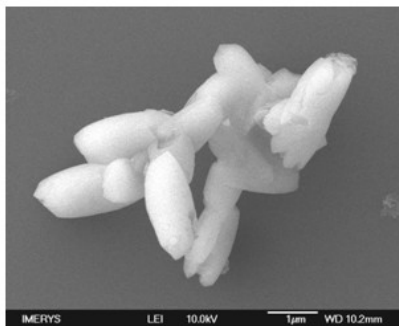
aPCC B (1.6 / 68 / 7.5)



aPCC C (2.3 / 69 / 6.0)



rPCC A (0.8 / 64 / 6.8)



rPCC B (1.3 / 66 / 4.4)

Figure 12a. Reflection spectra and opacity of scalenohedral PCC filled sheets

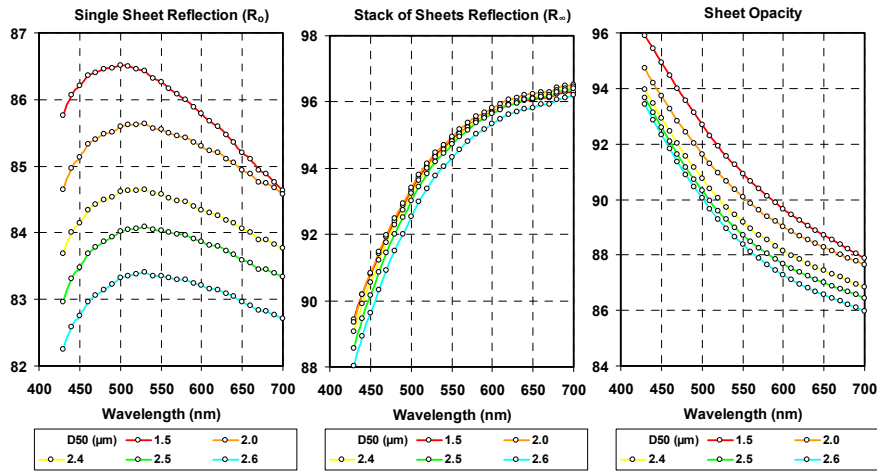


Figure 12b. Reflection spectra and opacity of aragonitic PCC filled sheets

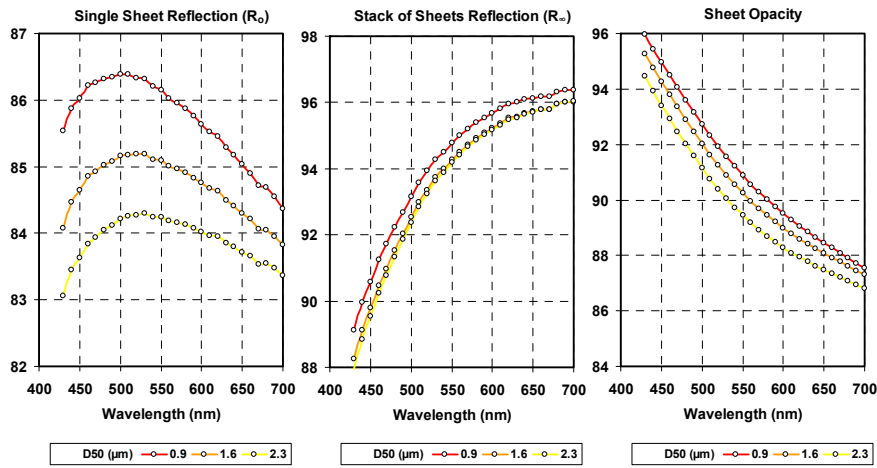


Figure 12c. Reflection spectra and opacity of rhombohedral PCC filled sheets

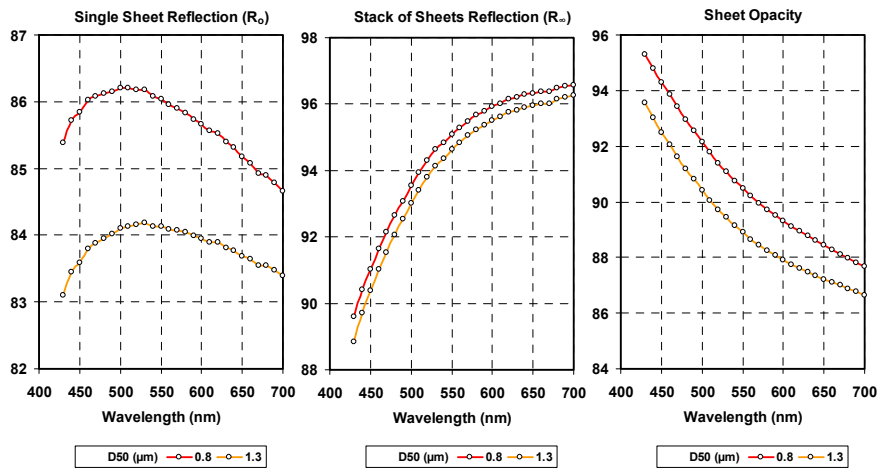


Figure 13a. Variation of sheet S and K with wavelength for scalenohedral PCC filled sheets

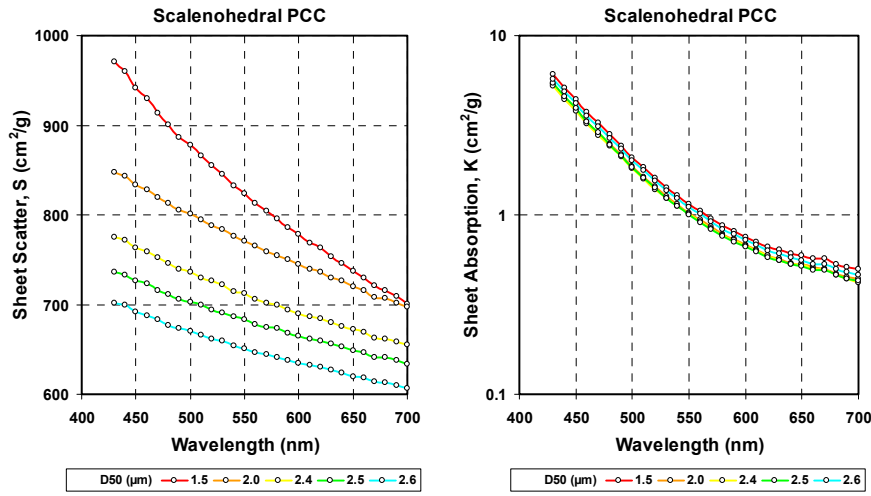


Figure 13b. Variation of sheet S and K with wavelength for aragonitic PCC filled sheets

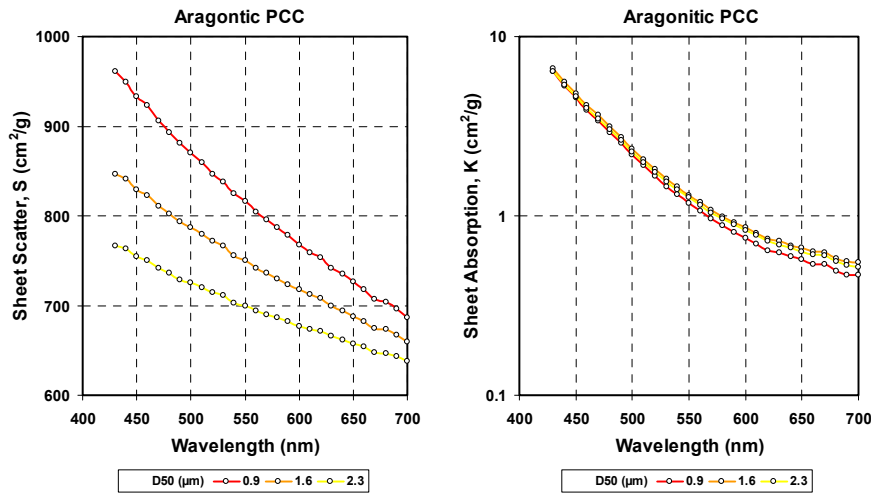


Figure 13c. Variation of sheet S and K with wavelength for rhombohedral PCC filled sheets

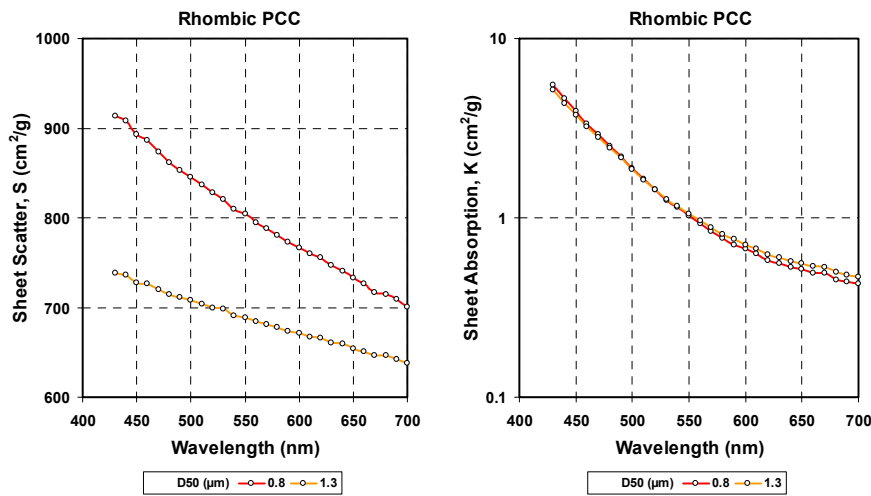


Figure 14. CIE colour parameters for PCC filled paper over solid print areas. The arrows indicate the trends when moving from finer to coarser PCC fillers.

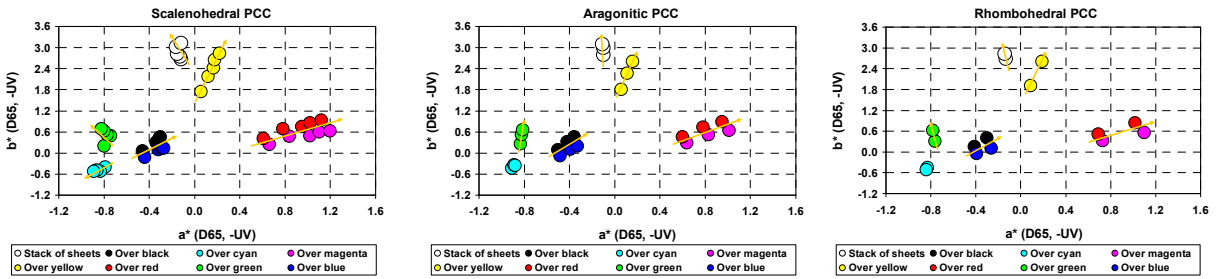


Figure 15a. The CIE-94 colour differences of the PCC filled papers over various printed colours.

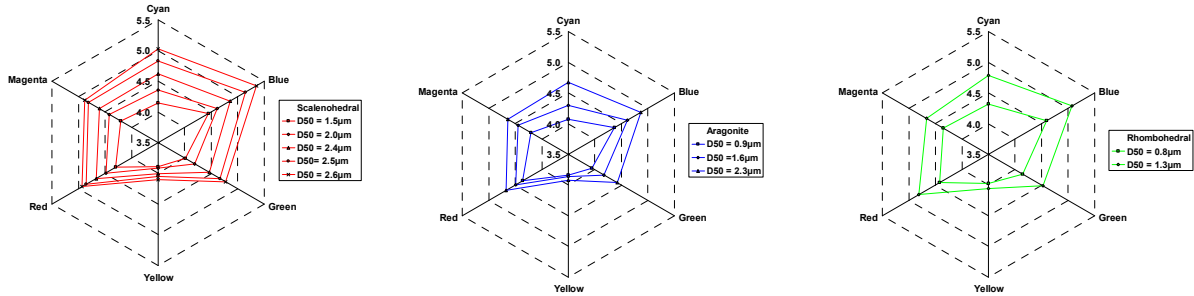


Figure 15b. The CIE-94 colour differences of the PCC filled papers over various printed colours.

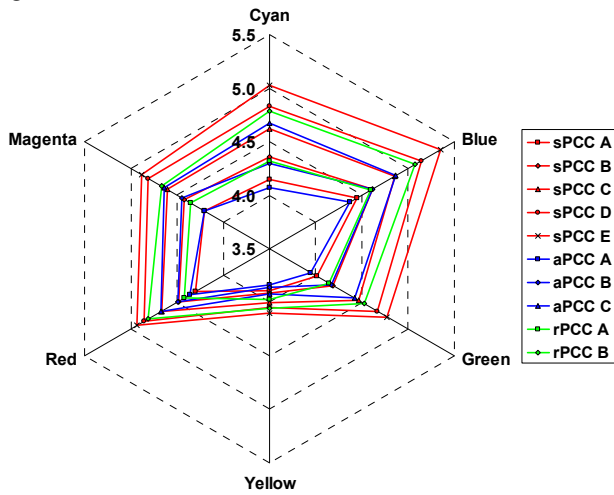
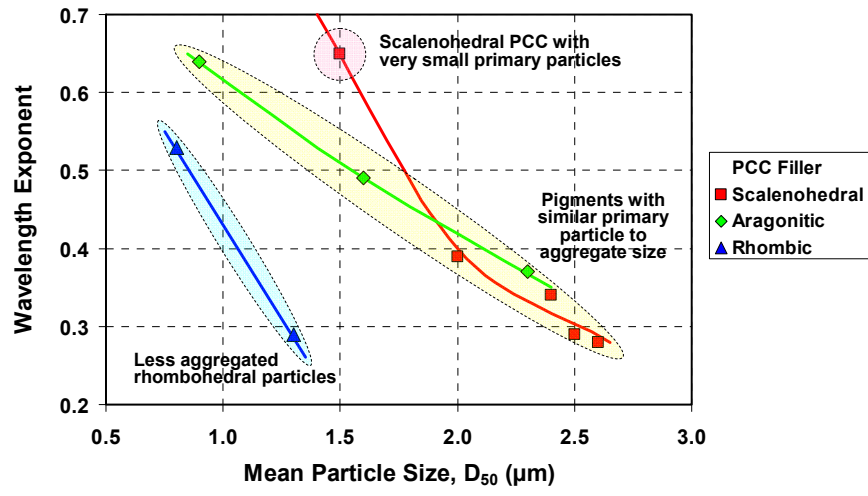


Figure 16. Relationship between wavelength exponent and mean aggregate particle size for PCC filled papers.





✦ **Europe**  
Tel: +44 1726 818000

✦ **Asia Pacific**  
Tel: +65 67 99 60 60

✦ **N. America**  
Tel: +1 770 594 0660

✦ **S. America**  
Tel: +55 11 2133 0055

**Email**  
[paper@imerys.com](mailto:paper@imerys.com)